

**Supplementary Materials:**  
**Ordinal partition transition network based complexity measures for inferring coupling  
direction and delay from time series**

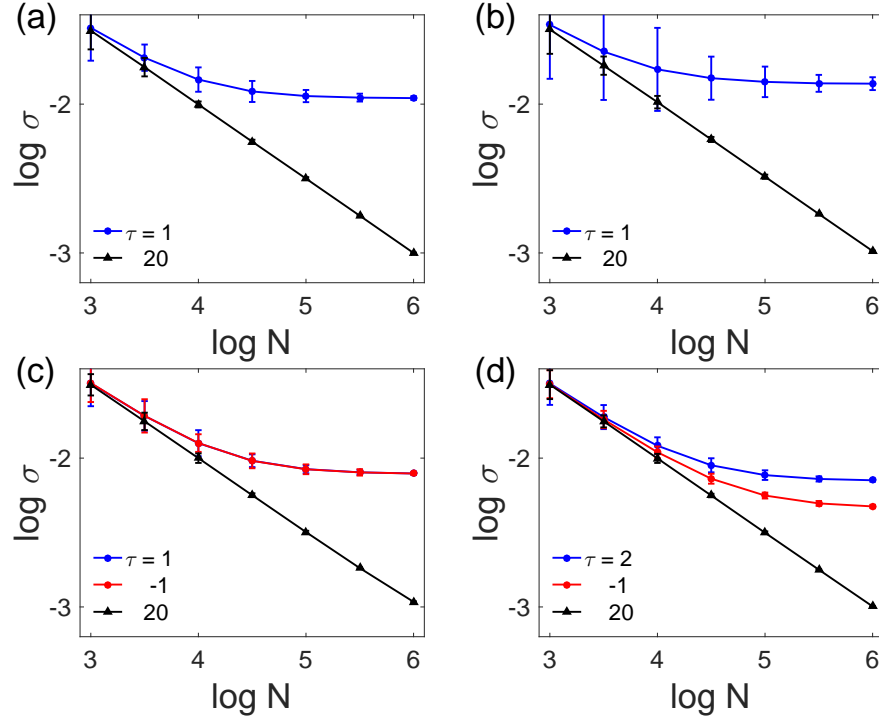


FIG. S1: Double logarithmic plot of the dependence of  $\sigma_{X \rightarrow Y}$  on the sample size  $N$  for the optimal (causal) lags (blue/red) and some non-causal lag (black) for the four cases of coupled linear-stochastic systems studied in the main paper: (a) Eq. (1) (unidirectional), (b) Eq. (9) (unidirectional), (c) Eq. (10) (symmetric bidirectional), (d) Eq. (11) (asymmetric bidirectional). In (c,d), the values for both causal delays are shown. Error bars indicate the associated standard deviation (in linear scale) over 20 independent realizations.

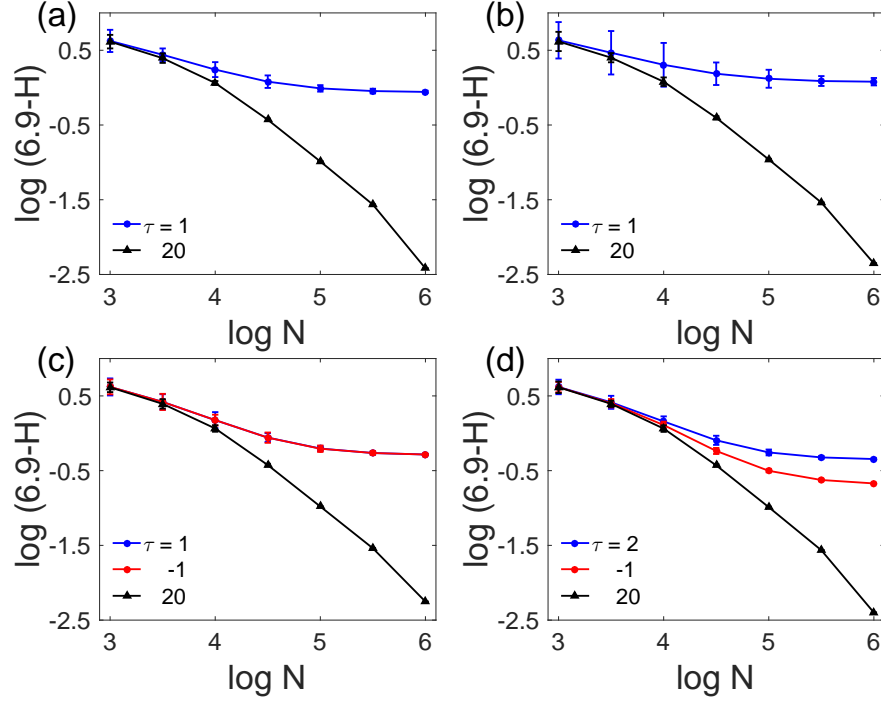


FIG. S2: Same as Fig. S1, but for the co-occurrence entropy  $H_{X \rightarrow Y}(\tau)$ . Note that for  $D = 5$ , we expect a co-occurrence entropy  $H_{X \rightarrow Y} \approx \log_2(5!) \approx 6.9$  for two series of ordinal patterns that are obtained from two independent identically distributed noise processes. Considering this fact, we show the difference between our estimated  $H_{X \rightarrow Y}$  values and that maximum value of 6.9, which yields similar asymptotic results as those for  $\sigma_{X \rightarrow Y}$  and KLD. Notably, at the positions of non-causal delays, zero values of the aforesaid difference are expected asymptotically, while non-zero values appear at the positions of causal delays.

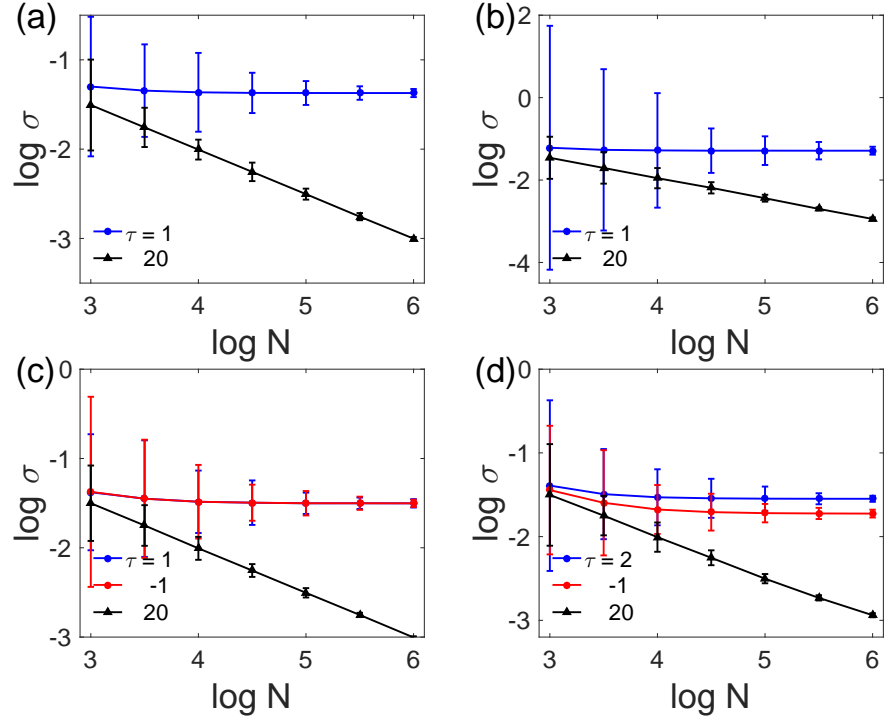
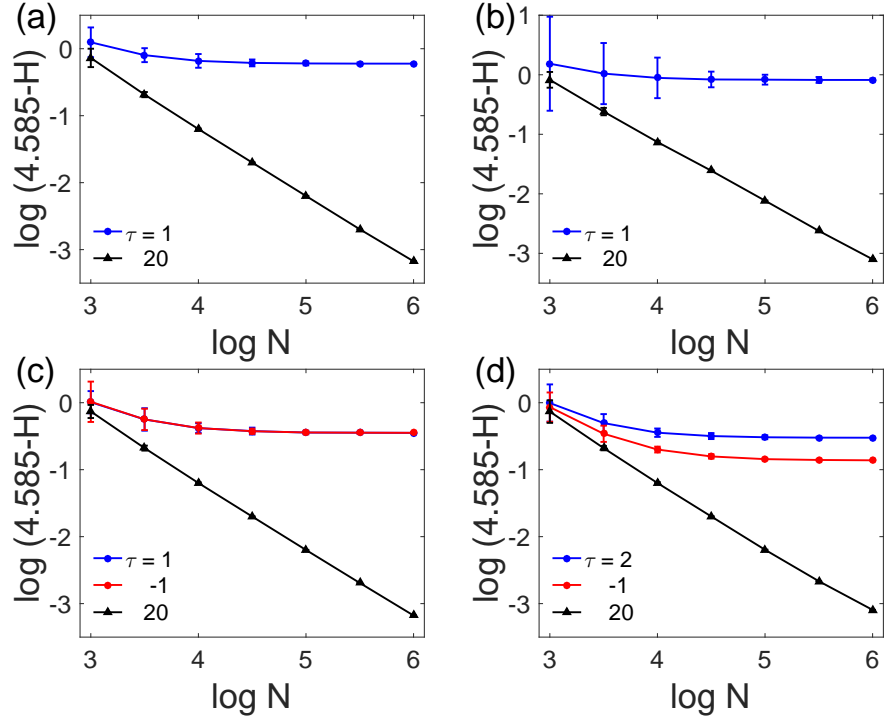
FIG. S3: Same as Fig. S1, but for  $D = 4$ .

FIG. S4: Same as Fig. S2, but for the  $H_{X \rightarrow Y}(\tau)$  and  $D = 4$ . Note that we expect a co-occurrence entropy  $H_{X \rightarrow Y} \approx \log_2(4!) \approx 4.585$  for two series of ordinal patterns that are obtained from two independent identically distributed noise processes.

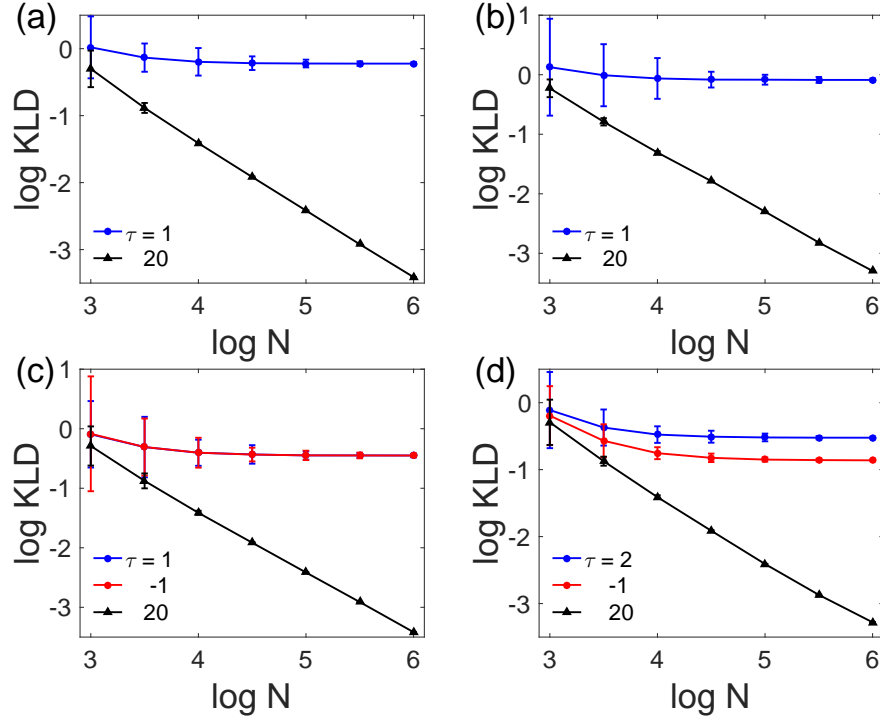


FIG. S5: (Color online) Same as Fig. S1, but for the KLD and  $D = 4$ .

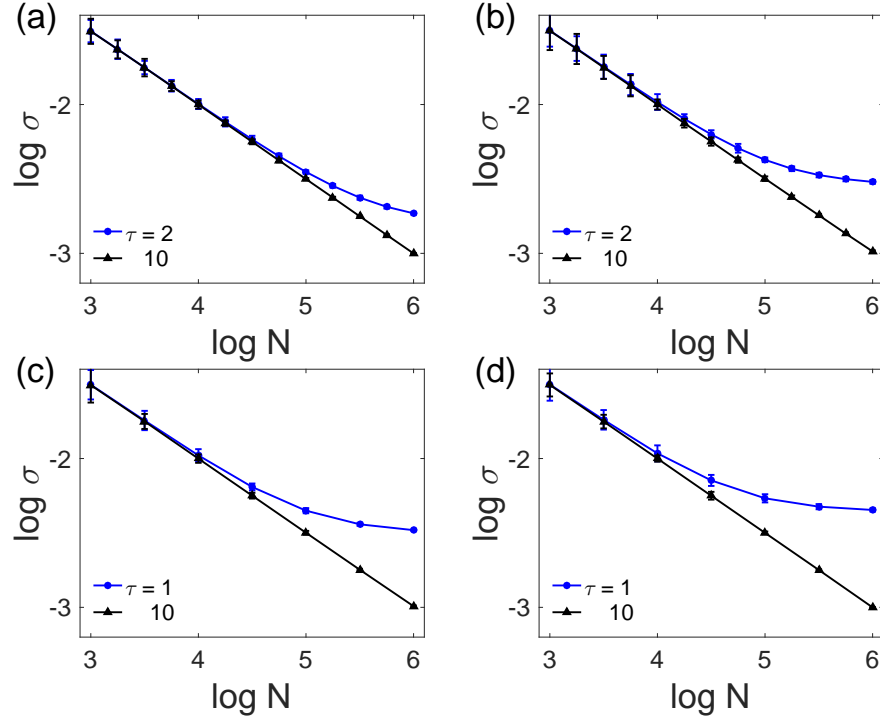


FIG. S6: Same as in Fig. S1 but for two coupled Hénon maps at four different coupling strengths  $\mu$ : (a)  $\mu = 0.2$  (b) 0.3, (c) 0.4, and (d) 0.5. The blue lines show the behavior at the delay corresponding to the maximum value of  $\sigma_{X \rightarrow Y}$ , while the black ones show the values for a non-causal delay of  $\tau = 10$ .

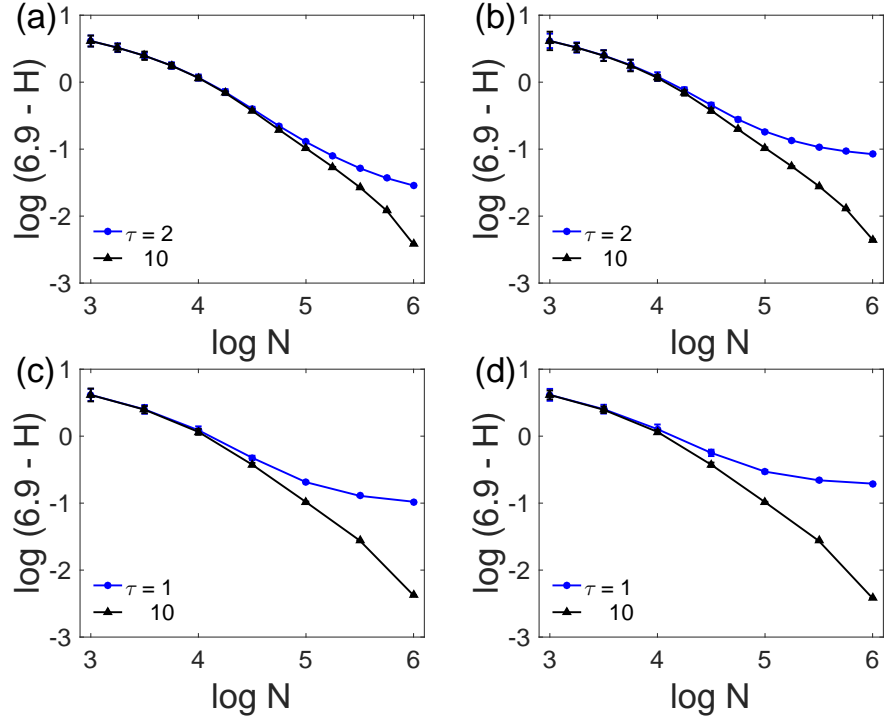


FIG. S7: Same as Fig. S6, but for the co-occurrence entropy  $H_{X \rightarrow Y}(\tau)$ .

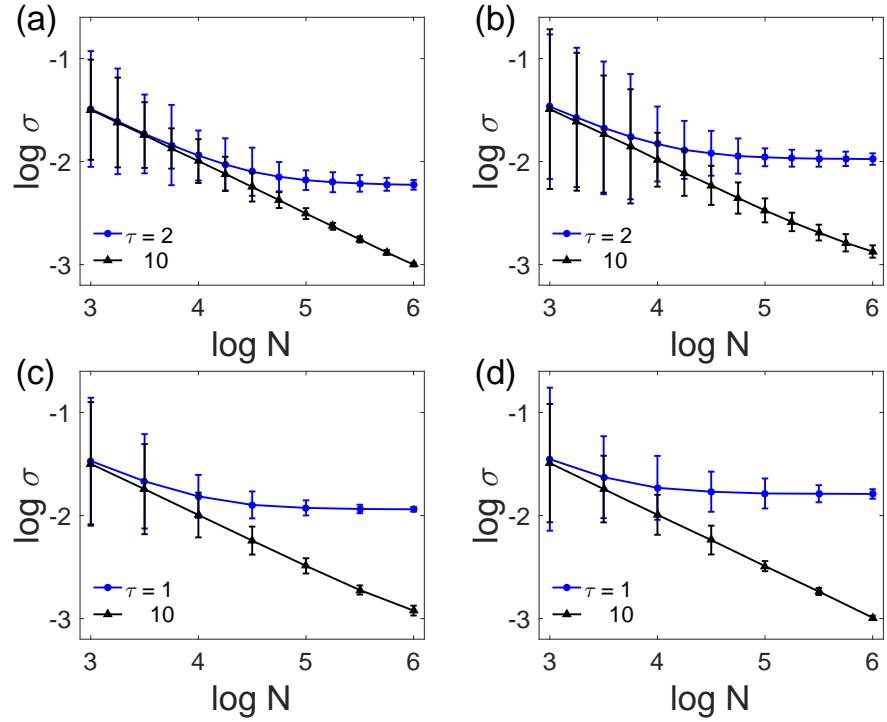


FIG. S8: Same as in Fig. S6 but for  $\sigma_{X \rightarrow Y}$  and  $D = 4$ .

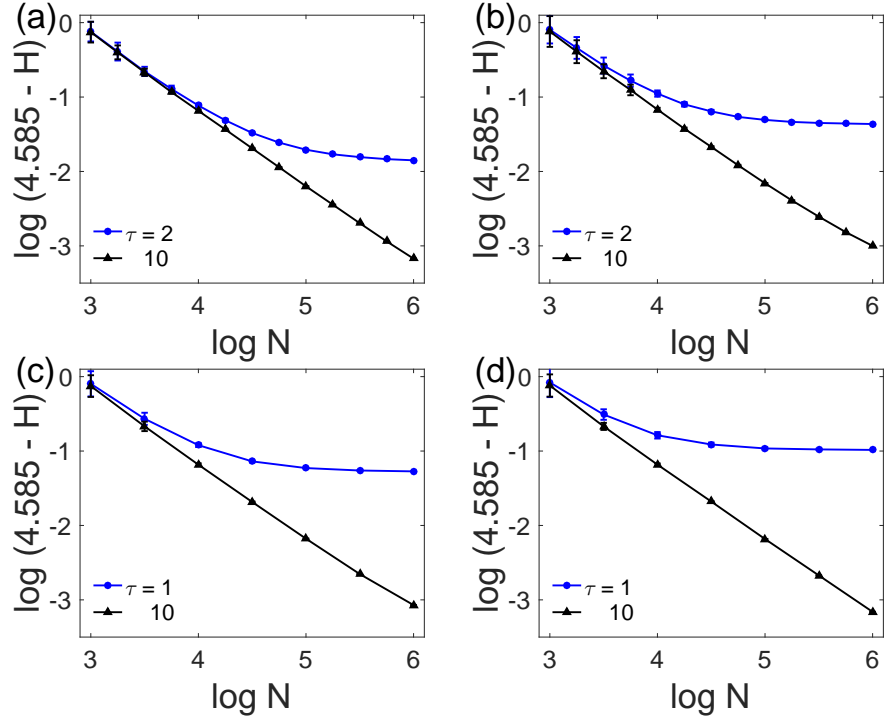


FIG. S9: Same as in Fig. S6 but for  $H_{X \rightarrow Y}$  and  $D = 4$ .

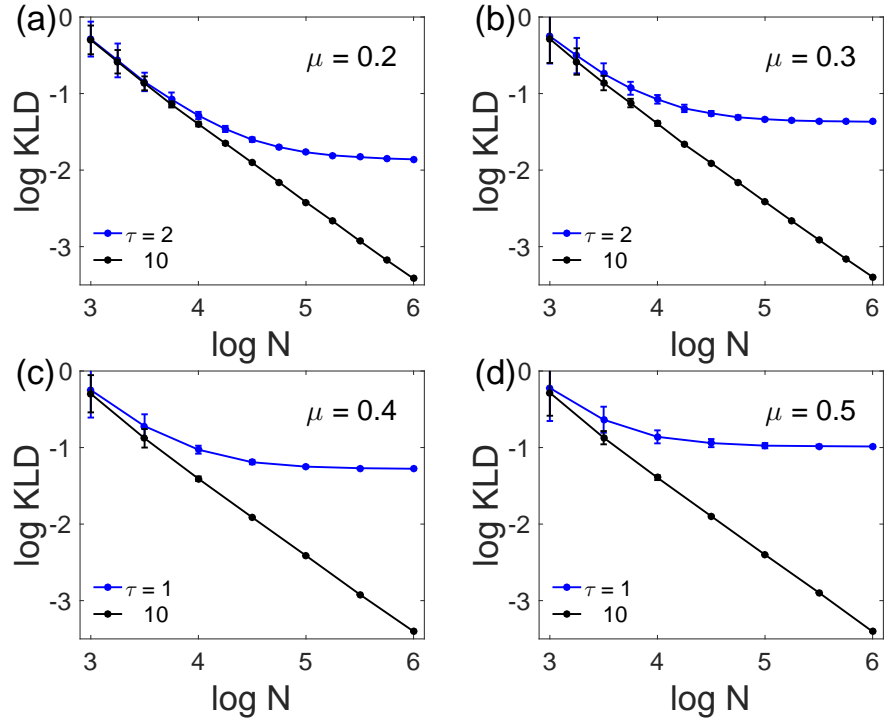


FIG. S10: Same as in Fig. S6 but for KLD and  $D = 4$ .

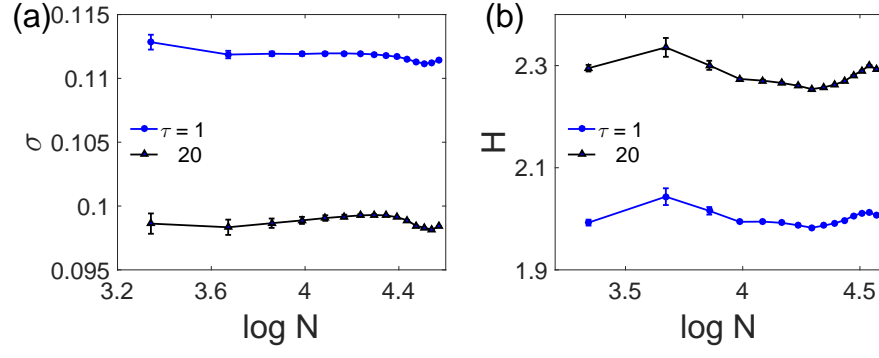


FIG. S11: Dependence of (a)  $\sigma_{X \rightarrow Y}$  and (b)  $H_{X \rightarrow Y}$  on the sample length  $N$  at the optimal delay ( $\tau = 1$  day, blue) and some arbitrarily chosen large delay ( $\tau = 20$  days, black) for the real-world example of two temperature time series from Oxford ( $X$ ) and Vienna ( $Y$ ) as discussed in the main text.